JOC The Journal of Organic Chemistry

Article

pubs.acs.org/joc

High Chemoselectivity of an Advanced Iron Catalyst for the Hydrogenation of Aldehydes with Isolated C=C Bond: A Computational Study

Xi Lu,[†] Runjiao Cheng,[‡] Nicholas Turner,[§] Qian Liu,[†] Mingtao Zhang,*[,‡] and Xiaomin Sun*[,∥]

[†]Department of Chemical and Materials Engineering, University of Alberta, Edmonton, Alberta T6G 2 V4, Canada

[‡]Computational Center for Molecular Science, College of Chemistry, NanKai University, Tianjin 300071, People's Republic of China

[§]Department of Chemical Engineering, Purdue University, West Lafayette, Indiana 47907, United States

[∥]Environment Research Institute, Shandong University, Jinan 250100, People's Republic of China

Supporting Information

ABSTRACT: Knölker's iron complex is a "green" catalyst that exhibits low toxicity and is abundant in nature. Density functional theory (DFT) was used to explore the highly chemoselective nature of the catalytic hydrogenation of CH_2=$CHCH_2CHO$. An outer-sphere concerted hydrogen transfer was found to be the most reasonable kinetic route for the hydrogenation of the olefin. However, the C=C hydrogenation reaction has a high free energy barrier of 28.1 kcal/mol, requiring a high temperature to overcome. By comparison, the CH=O bond concerted hydrogen-transfer reaction catalyzed using Knölker's iron catalyst has an energy barrier of only 14.0 kcal/mol. Therefore, only the CH=O of CH_2=$CHCH_2CHO$ can be hydrogenated in the presence of Knölker's catalyst at room temperature, due to kinetic domination. All computational results were in good agreement with experimental results.

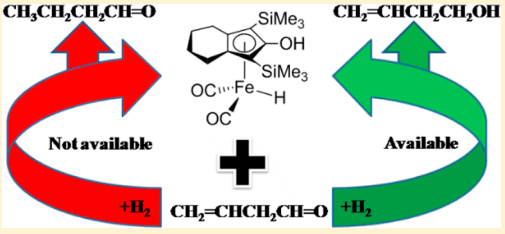

INTRODUCTION

Catalysis of bond-forming reactions by homogeneous transition metal complexes has proven to be an indispensable means in organic synthetic chemistry.[1] Since the discovery of Shvo's catalyst in the mid-1980s,[2] ligand precious metal (Ru, Rh, Ir, and Os) bifunctional catalysts have become potent substitutes for reducing agents such as $LiAlH_4$ and $NaBH_4$ for hydrogenation of olefin and carbonyl groups[3−5] due to their higher catalytic efficiencies.[6] As the first successful catalyst, Shvo's Ru complex, a (hydroxylcyclopentadienyl)diruthenium bridging hydride (Scheme 1), was applied to a broad scope of

Scheme 1. Shvo's Ligand Metal Bifunctional Catalyst

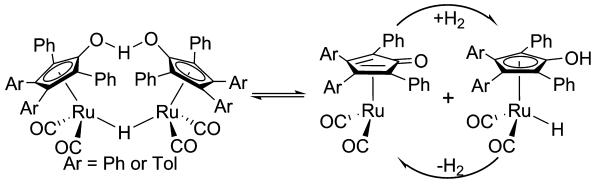

hydrogen-transfer reactions such as the hydrogenation of alkynes, carbonyls, and imines and the oxidation of alcohols, amines, and other compounds.[7−13]

However, sensitivity, toxicity, and high price seriously limit the availability of the noble-metal catalyst in industry.[14,15] By contrast, the "green" iron-based catalyst possesses some outstanding features such as low cost, low toxicity, and high natural abundance.[16,17] A stable and active iron-based complex is useful and valuable for the catalytic hydrogen transfer of unsaturated bonds. Particularly selective olefin and carbonyl hydrogenation are important transformations in the synthesis of chemicals, finding application in a wide range of substrates and functionalities.[18,19]

At the beginning of 1990s, Bianchini and co-workers investigated the hydrogen transfer of α,β-unsaturated ketones catalyzed by a trihydride iron complex **A**, $(PP_3)FeH(H_2)$-BPh_4(PP_3=$P(CH_2CH_2PPh_2)_3$) (Scheme 2).[20,21] This iron catalyst demonstrates a high selectivity for either the C=C or C=O bond in the presence of 2-propanol or cyclopentanol as a hydrogen donor, but the hydrogenated products are unpredictable. Notably, using alcohol as the hydrogen source is much more expensive than using H_2. Bhanage and co-workers successfully hydrogenated selectively the C=C bond of α,β-unsaturated carbonyl compounds in a biphasic medium using water-soluble Fe^{II}/Na_2EDTA as a catalyst (Scheme 3).[22] Recently, Chirik and co-workers developed a novel dimeric iron−nitrogen complex **E** by reduction of $(PDI)FeBr_2$ with sodium naphthalenide, which showed higher activity for the selective hydrogenation of C=C in ethyl-3-methylbut-2-enoate (Scheme 4).[23]

For the important C=O hydrogenation, Casey and Guan in 2007 reported the first application of Knölker's iron-based catalyst to the reduction of aldehydes and ketones.[24] Knölker's catalyst[25] was demonstrated to have an especially high

Received: August 21, 2014
Published: September 15, 2014

   dx.doi.org/10.1021/jo501946k | J. Org. Chem. 2014, 79, 9355−9364

Scheme 2. Reduction of α,β-Unsaturated Ketones in the Presence of a Trihydride Iron Complex Used by Bianchini and Co-Workers

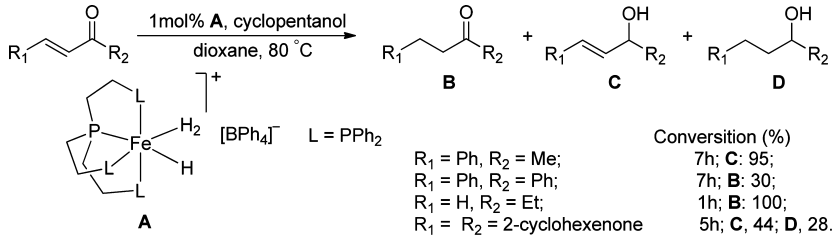

Scheme 3. Hydrogenation of α,β-Unsaturated Carbonyl Compounds Catalyzed by Fe^{II}/Na_2EDTA

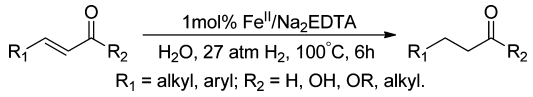

Scheme 4. Reduction of Ethyl-3-methylbut-2-enoate Catalyzed by Chirik's Iron Complex

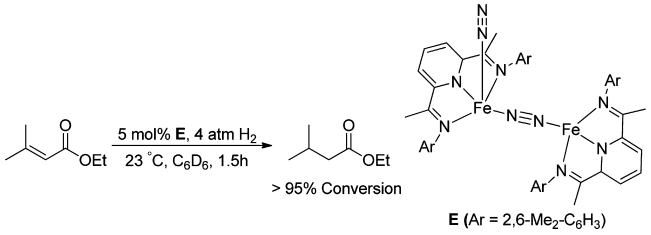

chemoselectivity for the C═O hydrogenation of aldehydes and ketones with isolated C═C bonds at room temperature and under low H_2 pressure (Scheme 5).

Scheme 5. Hydrogenation of Unsaturated Ketones with Isolated C═C Bonds Catalyzed by Knölker's Catalyst (Hydrogenation Is Faster in Toluene)

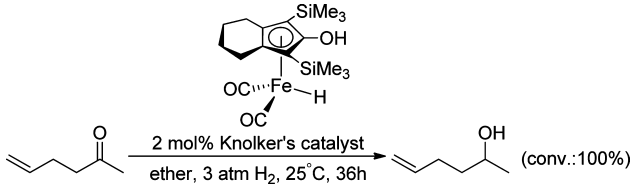

Currently, the reported iron-catalyzed reactions are still far off from real applications in industry, and the range of possible substrates should be further explored. Here, a deep and detailed exploration of the mechanisms and the elementary steps involved with the use of iron catalyst is offered as a prerequisite for the further improvement of iron catalysts. Density functional method was used to perform a thorough theoretical study for the selective hydrogenation catalyzed by Knölker's iron complex. This catalyst has a wide application prospect due to its chemical stability and facile synthetic route. The calculated results were then analyzed to clarify relationships between structures and actions in order to supply valid information to experiment.

RESULTS AND DISCUSSIONS

As Scheme 6 shows, there are four potential hydrogenations for CH_2═$CHCH_2CH$═O catalyzed by Knölker's catalyst in the presence of H_2. Reaction (i) indicates that the C═C bond of

Scheme 6. Some Possible Hydrogenations of CH_2═$CHCH_2CHO$ Catalyzed by Knölker's Catalyst

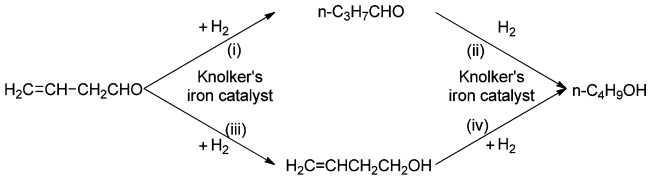

CH_2═$CHCH_2CHO$ is hydrogenated first. Reaction (ii) is the C═O hydrogenation of n-C_3H_7CHO, which is the product of reaction (i). Conversely, in reaction (iii) the C═O bond of CH_2═$CHCH_2CHO$ is hydrogenated first. Then, in reaction (iv), the C═C hydrogenation of CH_2═$CHCH_2CH_2OH$, which is the product of reaction (iii), takes place. Reactions (i) and (iii) are two chemically competitive reactions, where either C═C or C═O of CH_2═$CHCH_2CHO$ is hydrogenated by the iron catalyst. Reactions (ii) and (iv) are further hydrogenations of the products of (i) and (iii). According to experimental studies, Knölker's catalyst shows a very high chemical selectivity for hydrogenation of aldehydes with isolated C═C, meaning that only (iii) could occur in experiments, without further hydrogenation of its product. Here, all of these hydrogenations were analyzed in detail via computational methods in order to investigate this feature of Knölker's catalyst.

Inner-Sphere Coordinated Hydrogenation Route for Olefin of CH_2═$CHCH_2CHO$. To the best of our knowledge, there has not been theoretical and experimental research on the hydrogenation mechanism of olefin catalyzed by Knölker's catalyst. So, it is necessary to first study the C═C hydrogenation. According to Chirik and co-workers,[26,27] the olefin is most likely hydrogenated by means of a coordinated catalysis. Here we explore two routes, which separately generate a vacant site using five-member ring slippage and CO leaving. The entire aromatic ligand of catalyst **1** is hereafter referred to as CpOH.

In the first route, the olefin binds to the iron center via a $\eta^5 \rightarrow \eta^2$ slippage of a CpOH ring (as shown in Scheme 7). Following the C═C coordination, olefin insertion forms a β-H agostic intermediate state **3**. Then oxidative addition of H_2 achieves an 18-electron olefin dihydride intermediate state **4**. Finally, intramolecular hydrogen migration and subsequent alkane reductive elimination result in the product, n-butyraldehyde, and the regenerated catalyst **1**.

Figure 1 shows that the free energy barrier $\Delta G^{\ddagger}$(sol) is 51.1 kcal/mol for **1** + CH_2═$CHCH_2CHO$ → **2**. In the transition state **1/2TS** of this step, distances between C═C bond and iron centers are 2.731 and 2.889 Å (see Figure 2), respectively, which indicates that the π electrons of the CH_2═CH bond are coordinating to the iron center of catalyst **1**. Due to the CH_2═

dx.doi.org/10.1021/jo501946k | J. Org. Chem. 2014, 79, 9355−9364

Scheme 7. Catalytic Hydrogenation of the C═C Bond According to Chirik's Proposed Mechanism

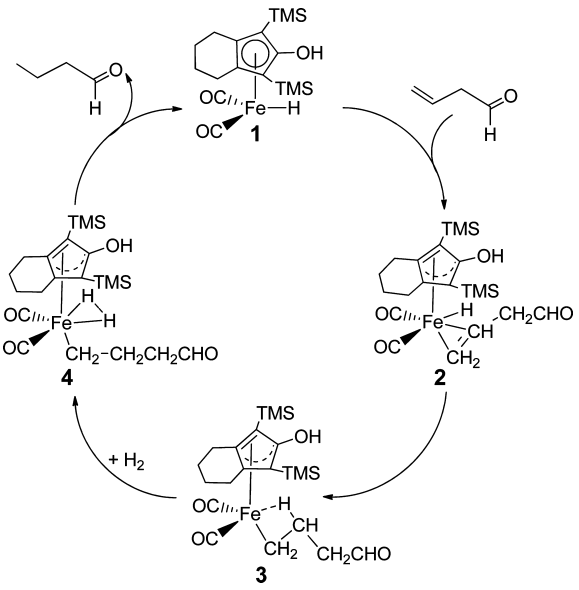

CH coordination interaction, three carbon atoms of the CpOH ring must be removed from the iron center by means of upward slipping. Thus, the π-coordinated CH_2═CH bond partially replaces the original CpOH ring ligand. This reaction produces an intermediate state **2,** which is endergonic by 50.2 kcal/mol. Considering the high reactivity of intermediate **2**, it was very simple to form a more thermodynamically stable intermediate **3** using transition state **2/3TS**. Because the free energy barrier was only 0.3 kcal/mol, this process occurred very rapidly. This is actually an intramolecular hydrogen-transfer reaction, where the proton migrates from iron to one carbon atom of the C═C bond. An intermediate state **3**, which exhibits a strong, agnostic hydrogen interaction due to the 1.827 Å H···Fe distance, was then obtained in this step.

Although it is exergonic by −9.4 kcal/mol for **2** → **3**, the free energy ΔG(sol) of **3** is still 40.8 kcal/mol compared to the original reactants. This indicates that **3** is also a highly active intermediate state. Therefore, H_2 easily added to the iron of intermediate state **3** via transition state **3/4TS** with a free energy barrier of only 2.2 kcal/mol. Distances of H_2···Fe are 2.524 and 2.660 Å in the structure of **3/4TS**, which means that the two H atoms are concertedly coordinating to intermediate state **3**. This additive reaction led to a η^2-H_2 coordinated complex **4**, which was endergonic by 6.0 kcal/mol. Finally, an intramolecular hydrogen addition occurs via transition state **4/1TS**, which gives regenerated catalyst **1** and the hydrogenated product C_3H_7CHO. In this process, one coordinated hydrogen transfers to the carbon atom of Fe−C(aldehyde) from the iron center, a step that has a free energy barrier of 3.3 kcal/mol. The step of **4** → **1** + *n*-C_3H_7CHO is highly exergonic (by 73.6 kcal/mol), which indicates that this hydrogen transfer is thermodynamically favorable in dihydride complex **4**.

Overall, this route achieves the hydrogenation of olefins involving highly active intermediate states. As Figure 3 shows, the highest free energy is the 51.1 kcal/mol of transition state **1/2TS**. Thus, the rate-determining step corresponds to a step where the olefin adds to the iron center and the CpOH ring slips from η^5- to η^2-coordination simultaneously. The highest free energy barrier was also 51.1 kcal/mol for this hydrogenation route, which is kinetically unfeasible at room temperature.

Inner-Sphere Stepwise Route for Olefin Hydrogenation. Due to the η^5-CpOH ring ligand having a very strong coordinating interaction with iron, the direct breaking of the Cp−iron coordination bonds must overcome a quite high free energy barrier. The second potential hydrogenation pathway of C═C is discussed in this section. Figure 3 presents the general pathway and free energy profiles. Here, one Fe−CO bond is broken in catalyst **1** prior to the C═C bond coordination. Next, the dissociation of the CO ligand generates an intermediate state **5** that has a vacant site in the iron center. The departure of the CO ligand of **1** was found to be a purely

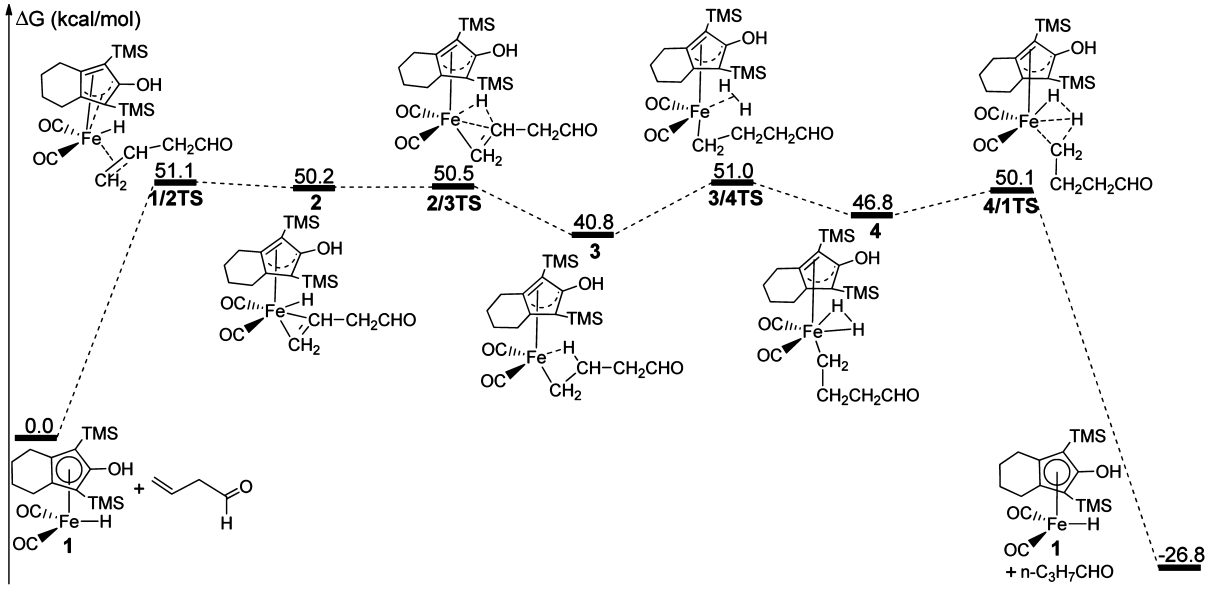

Figure 1. Free energy ΔG(sol) profiles for the inner-sphere coordinated hydrogenation of the reaction (i) were obtained at the M06/def2-TZVP,6-311+G* level in toluene (kcal/mol). These are relative to free energies of **1** and CH_2═$CHCH_2CHO$.

dx.doi.org/10.1021/jo501946k | J. Org. Chem. 2014, 79, 9355−9364

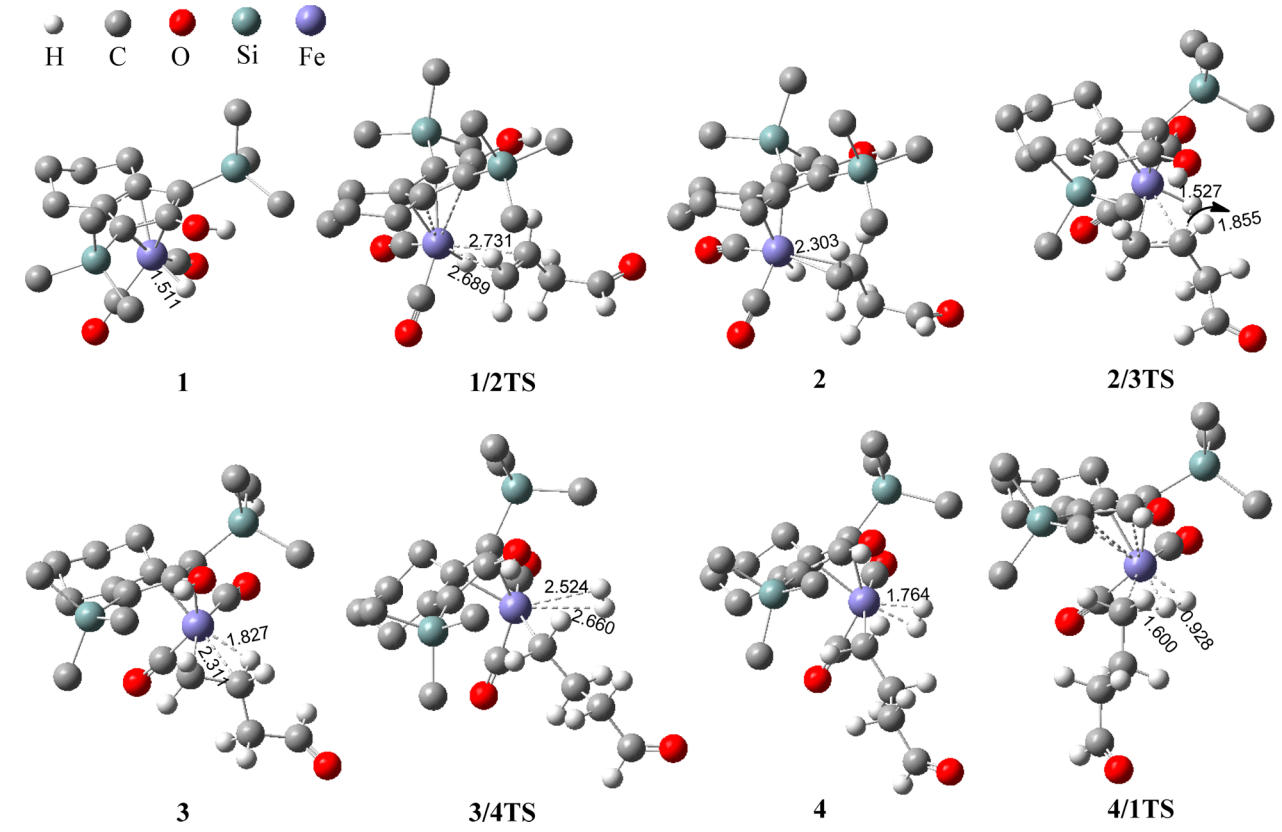

Figure 2. Located stationary points in the ring slippage mechanism. Distances are in Å.

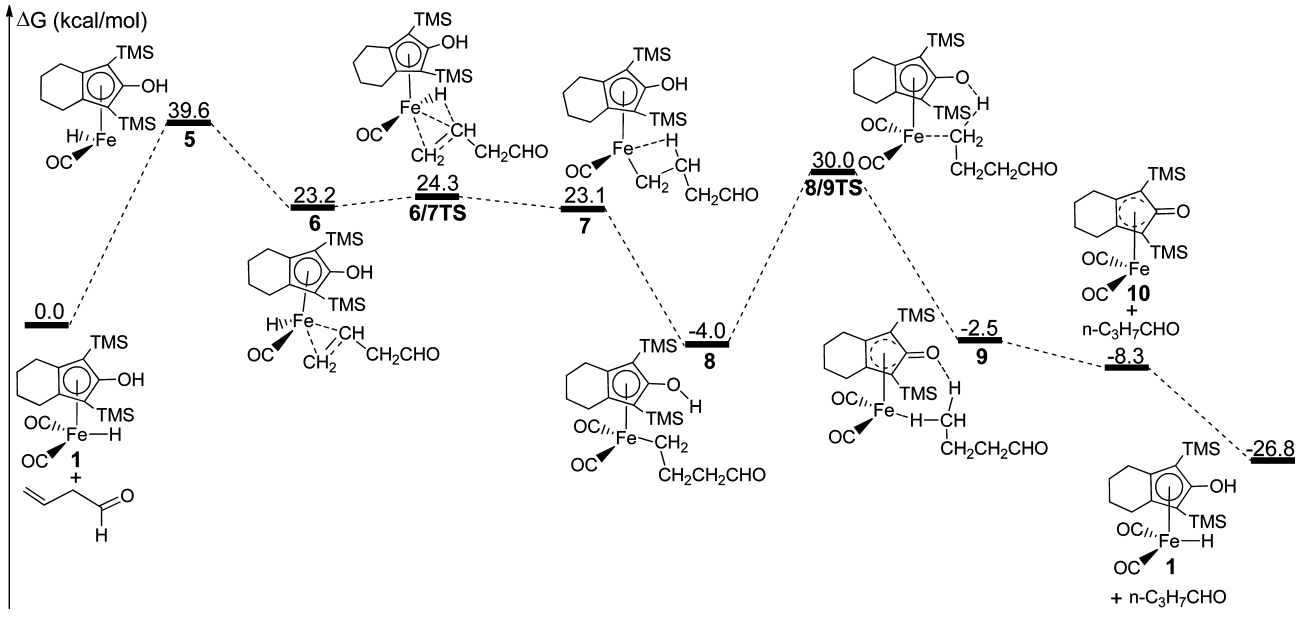

Figure 3. Free energy ΔG(sol) profiles for the inner-sphere stepwise hydrogenation of reaction (i) in toluene (kcal/mol). These are relative to free energies of **1** and CH_2═$CHCH_2CHO$.

endergonic process on the potential surface without the transition state. Although this dissociation is to some extent entropically favored, the calculated ΔG(sol) is still large: 39.6 kcal/mol. This is because the unsaturated iron complex **5** is not able to satisfy the 18-electron structure of iron and causes an extreme decrease in thermodynamic stability.

The generated vacant site is then occupied by the olefin to obtain intermediate **6**, while releasing 16.4 kcal/mol of energy. Figure 4 shows that two Fe−C(olefin) bond lengths are 2.096 and 2.118 Å in the geometry of **6**. This indicates that the CH_2═$CHCH_2CHO$ forms a η^2-coordinated interaction with the iron center using π-electrons of the olefin. However, intermediate **6** still has a high free energy of 23.2 kcal/mol in comparison to the original reactants. Due to **6** exhibiting high reactivity, it is very easy to perform an intramolecular hydrogen transfer using the transition state **6**/**7TS**. In the structure of **6**/

dx.doi.org/10.1021/jo501946k | J. Org. Chem. 2014, 79, 9355−9364

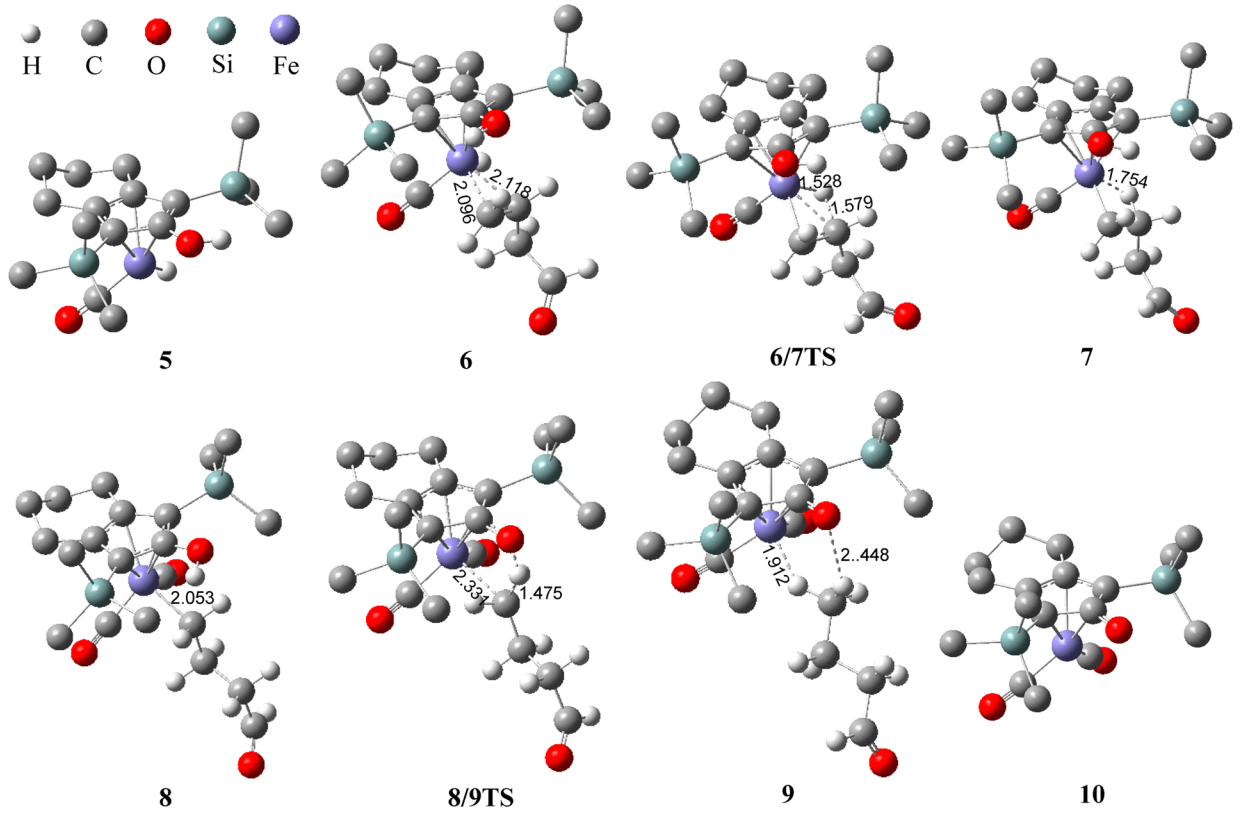

Figure 4. Located stationary points in the inner-sphere stepwise hydrogenation. Distances are in Å. All hydrogen atoms connected to carbons in the CpOH ring were ignored for all drawing geometries in this paper.

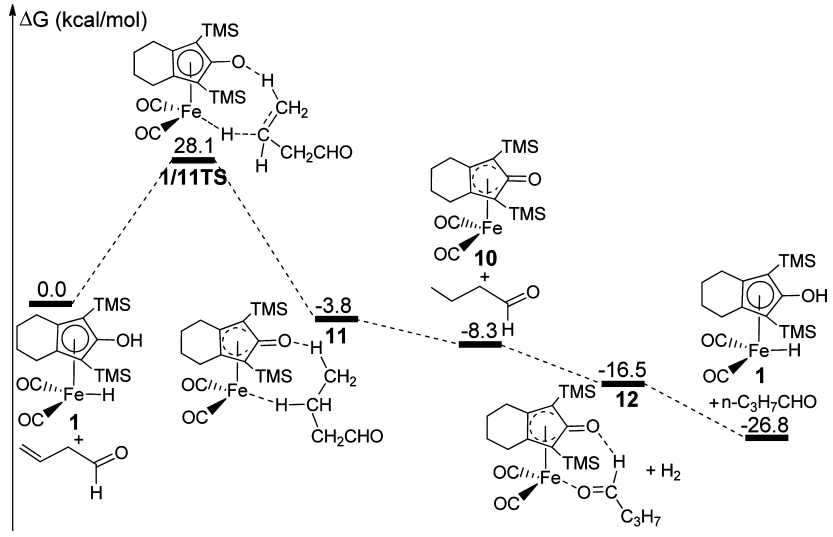

Figure 5. Free energy ΔG(sol) profiles for the concerted hydrogen-transfer route of reaction (i) in toluene (kcal/mol). These are relative to free energies of **1** and CH_2═$CHCH_2CHO$.

7TS, the Fe−H bond is 1.528 Å, which is very close to the 1.511 Å of catalyst **1**. The hydrogen atom easily migrates from iron to the carbon atom of the olefin with a free energy barrier of only 1.1 kcal/mol. This step also gave rise to a highly active intermediate **7**, which has a ΔG(sol) of 23.1 kcal/mol relative to **1** and CH_2═$CHCH_2CHO$.

Even though there is a β-H agostic interaction in intermediate **7** where the Fe···H distance was 1.754 Å, the iron atom does not achieve an 18-electron structure. Moreover, the agostic-H bond is a weak interaction and could be easily replaced by a carbonyl ligand coordination in order to obtain an alkyl iron complex **8**. In particular, our calculations show that there is a very flat potential surface with no barrier for CO coordination with the iron center. This is actually a spontaneous process without any barriers and is exoergic by 27.1 kcal/mol for **7** + CO → **8**. Next, the proton of the CpO−H group moves to the carbon atom of the alkyl−Fe bond through a transition state **8/9TS** with a free energy barrier of 34.0 kcal/mol. In the structure of **8/9TS**, the H···CH_2 distance shrank to 1.475 Å, whereas the CpO···H distance lengthened to

dx.doi.org/10.1021/jo501946k | J. Org. Chem. 2014, 79, 9355−9364

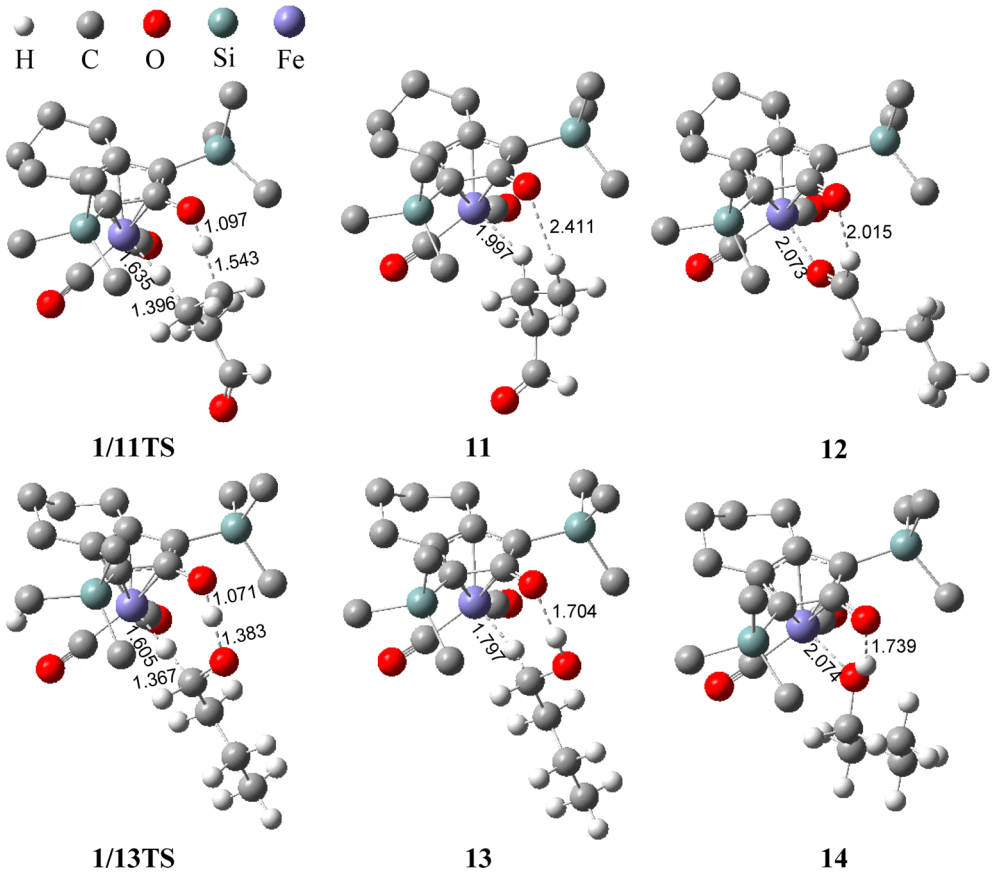

Figure 6. Optimized structures of reaction (i) and (ii) via a concerted hydrogen transfer. Distances are in Å.

2.331 Å. This indicates that the Fe−CH_2 bond is being broken during the electrophilic addition. This step gives rise to an intermediate **9**, which has an agostic interaction (1.912 Å for Fe···H distance) and an intramolecular hydrogen bond (2.448 Å for CpO···H−CH_2 distance). The Fe−CH_2 was also broken, and intermediate **9** remains thermodynamically stable. The calculated ΔG(sol) was only 1.5 kcal/mol for **8** → **9**. Finally, intermediate **9** dissociates to a dehydrogenated iron complex **10** and *n*-C_3H_7CHO, a process that is exoergic by 5.8 kcal/mol. In a H_2 environment, iron complex **10** is able to be regenerated to catalyst **1**.[24,28]

For this route, the highest free energy difference is 39.6 kcal/mol between the reactants of **1** + aldehyde and intermediate **9**, which corresponds to the CO leaving step. This is an obvious kinetic improvement compared to the CpOH ring slippage pathway (39.6 versus 51.1 kcal/mol). However, both inner-sphere routes are still kinetically unfavorable due to their high free energy barriers, owing to a large structural difference between Chirik's and Knölker's iron complex. The tridentate nitrogen is a weak-field ligand in Chirik's iron complex,[26,27,29] so the iron atom can generate various spin states that effectively render catalytic hydrogenation kinetically feasible even though the iron atom is not an 18-electron structure. Because the carbonyl group is a strong-field ligand in Knölker's catalyst, it causes the iron atom to remain in a ground state during the entire hydrogenation process.[30,31] So, Knölker's iron complex cannot catalyze C═C hydrogenation via the inner-sphere route.

Concerted Outer-Sphere Hydrogenation Route. On the basis of our previous research on catalytic hydrogenation of ketones, these substrates prefer to be hydrogenated by means of a concerted hydrogen transfer.[30] Considering the inner-sphere route being unavailable, the outer-sphere route was further explored for the hydrogenation of olefin. In this route, the proton and hydride transfers can be achieved simultaneously in a single step.

As shown in Figure 5, there is only one transition state **1/11TS** in the whole hydrogen transfer. The structure of **1/11TS** shows that the substrate is in close proximity to catalyst **1**, while H···CH_2 and H···CH distances were 1.543 and 1.396 Å, respectively (see Figure 6). Although it causes to some extent an entropic penalty through transition state **1/11TS**, the free energy barrier of 28.1 kcal/mol is lower than that of the inner-sphere routes. In intermediate **11**, respective Fe···H and O···H distances are 1.997 and 2.411 Å, which indicates an agostic interaction and a hydrogen bond, respectively. Both interactions improve upon the thermodynamic stability of geometry **11**, so the reaction of **1** + CH_2═$CHCH_2CHO$ → **11** is only exergonic by 3.8 kcal/mol. Then the iron complex **10** and C_3H_7CHO are obtained by further decomposition of **11**. Here, the free product C_3H_7CHO is able to reconnect to complex **10** using a hydrogen bond and an oxygen−iron coordination interaction, which effectively improves the thermodynamic stability of product **12**. The calculated ΔG(sol) of **1** + CH_2═$CHCH_2CHO$ → **12** was −16.5 kcal/mol. Finally, product **12** is regenerated to catalyst **1** and C_3H_7CHO under H_2 conditions.

For this outer-sphere route, the total free energy barrier is 28.1 kcal/mol. The rate-determining step corresponds to two hydrogen atoms concertedly adding to the olefin. Obviously, this pathway is more kinetically favorable for the hydrogenation of olefin compared to the two inner-sphere routes. Hydro-

dx.doi.org/10.1021/jo501946k | J. Org. Chem. 2014, 79, 9355−9364

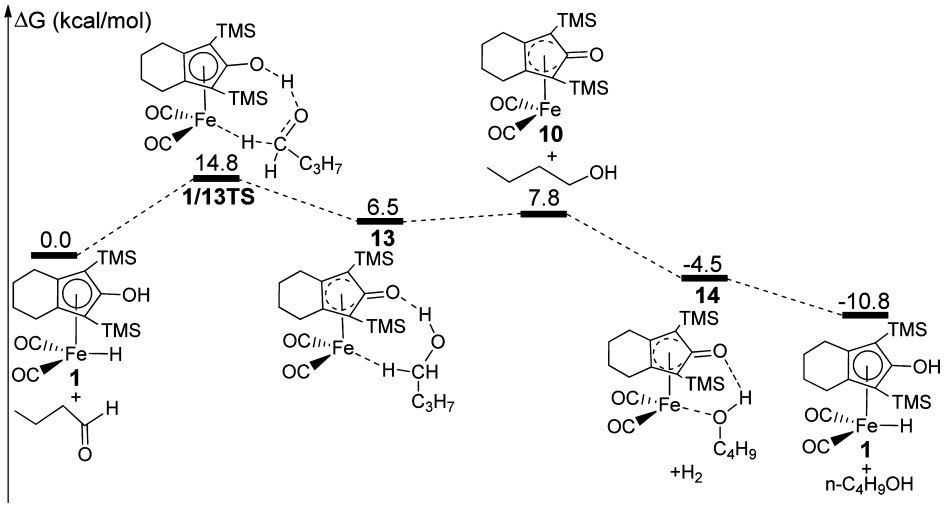

Figure 7. Free energy ΔG(sol) profiles for the carbonyl hydrogenation of reaction (ii) in toluene (kcal/mol). These are relative to the free energies of **1** and *n*-C_3H_7CHO.

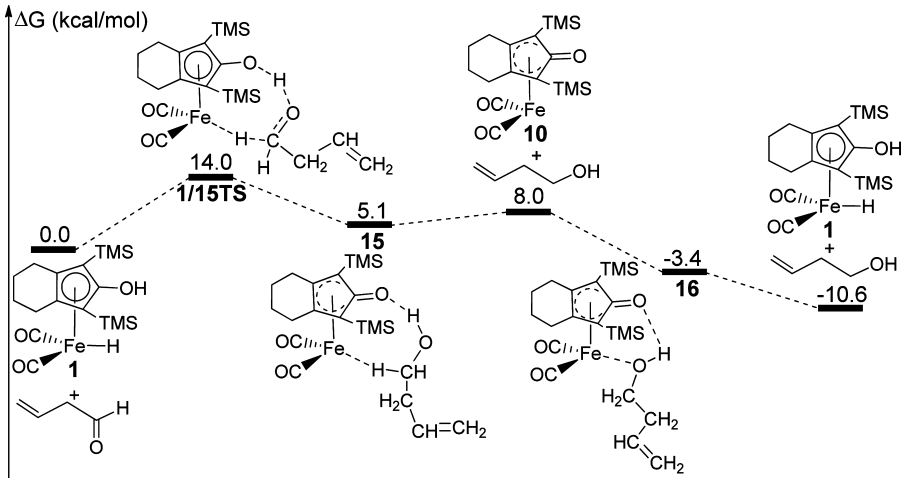

Figure 8. Free energy ΔG(sol) profiles for reaction (iii) (kcal/mol) in toluene. These are relative to the free energies of **1** and CH_2=$CHCH_2CHO$.

genation of the olefin is better catalyzed by Knölker's catalyst by means of an outer-sphere concerted hydrogen-transfer route.

However, hydrogenation is not going to stop here. According to our previous studies, the product *n*-C_3H_7CHO may be further hydrogenated by way of Knölker's catalyst.[30,32] The aldehyde also can be hydrogenated by Knölker's catalyst via the concerted outer-sphere hydrogenation pathway. Figure 7 shows that the total free energy barrier is only 14.8 kcal/mol for **1** + *n*-C_3H_7CHO → **14**. The structure of **14** is similar to that of **12**, but what the former has is special in that the product *n*-butanol is connected to iron complex **10** by a hydroxyl group. The CpO···HO distance shrank to 1.739 Å in complex **14** (Figure 6), because the OH group causes a stronger hydrogen-bond interaction compared to the CHO of complex **12**. Correspondingly, the thermodynamic stability of **14** is improved relative to that of complex **12** and is exergonic by 14.8 kcal/mol for **12** + H_2 → **14**. Further hydrogenation of C_3H_7CHO is kinetically and thermodynamically available. As presented above, reactions (i) and (ii) are actually a tandem hydrogenation process.

Carbonyl Hydrogenation of CH_2=$CHCH_2CHO$ via Reaction (iii). On the basis of the above computational results, if reaction (i) took place, the final product was actually obtained from the (ii) catalytic hydrogenation. Thus, it should be *n*-butanol rather than *n*-butyraldehyde if C=C hydrogenation occurred first. This was different from the experimental results, where only CH_2=$CHCH_2CH_2OH$ was obtained as product. However, 1-butenol was only produced through reaction (iii). To understand this, the carbonyl hydrogenation of CH_2=$CHCH_2CHO$ is calculated in this section.

For hydrogenation of aldehydes, an outer-sphere concerted hydrogen-transfer route had been demonstrated to be the most kinetically and thermodynamically favorable pathway in previous experimental and theoretical studies.[24,28,30] As shown in Figure 8, the substrate and catalyst **1** first interact to form intermediate **15** through transition state **1/15TS**, corresponding to a concerted hydrogen migration. A free energy barrier of 14.0 kcal/mol was calculated for this step. Intermediate **15** is a complex composed of **10** and an alcohol with an agostic interaction, where the Fe···H distance is 1.818 Å, and a hydrogen bond whose O···H distance is 1.703 Å (see Figure 9). Here, the iron atom was not able to satisfy an 18-electron structure, so the thermodynamic stability of **15** is reduced in comparison to catalyst **1**. It is endergonic by 5.1 kcal/mol for **1**+ CH_2=$CHCH_2CHO$ → **15**. The dissociation of **15** is slightly endergonic by 2.9 kcal/mol and results in **10** and the

dx.doi.org/10.1021/jo501946k | J. Org. Chem. 2014, 79, 9355−9364

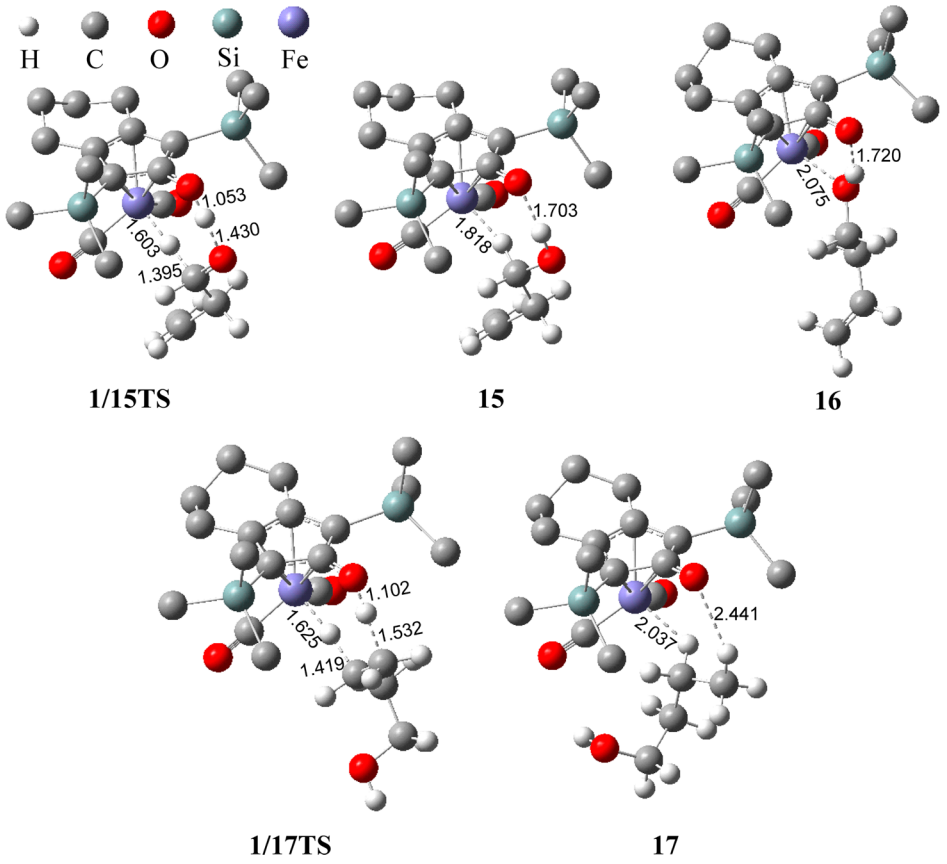

Figure 9. Optimized structures in reactions (iii) and (iv). Distances are in Å.

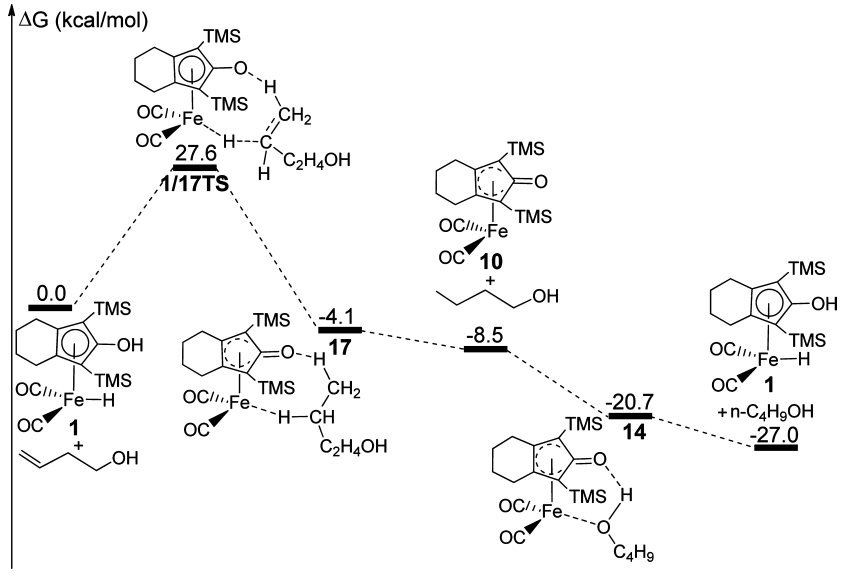

Figure 10. Free energy ΔG(sol) profiles for the C═C hydrogenation of reaction (iv) (kcal/mol) in toluene. These are relative to the free energies of **1** and CH_2═$CHCH_2CH_2OH$.

free 1-butenol. However, the separated **10** is also thermodynamically unstable and could easily reconnect to 1-butenol to form complex **16**. Distances of Fe···O and O···H are 2.075 and 1.720 Å, respectively, in the structure of **16**, which corresponds to a σ-coordinated interaction and a hydrogen bond between iron complex **10** and 1-butenol. **10** + CH_2═$CHCH_2CHO$ → **16** is exoergic by 11.4 kcal/mol. This calculation is very consistent with previous theoretical and experimental results.[23]

Hydrogenated product **10** could be regenerated to catalyst **1** through a reduction reaction in the presence of H_2.

Here the total free energy barrier is only 14.0 kcal/mol for the catalytic hydrogenation of aldehyde, where the determining step is a hydrogen-transfer process. This barrier is 14.1 kcal/mol lower than the 28.1 kcal/mol of the hydrogenation of an olefin. On the basis of the Eyring equation, $k = k_BT/h \times e^{-(\Delta G^{\ddagger}/RT)}$, the rate constant of hydrogenation of aldehyde was

dx.doi.org/10.1021/jo501946k | J. Org. Chem. 2014, 79, 9355−9364

improved by ~2.0×10^{10} times relative to the hydrogenation of olefins at 25 °C. The hydrogenation of aldehyde is kinetically more favorable in the presence of Knölker's catalyst and corresponds to a rapid reaction rate at room temperature, whereas hydrogenation of the olefin is kinetically unfeasible in this case. In this case the hydrogenation is completely dominated by kinetics. The aldehyde group can be hydrogenated prior to hydrogenation of the olefin when CH_2=$CHCH_2CHO$ is added to the solution of Knölker's catalyst in a H_2 environment.

To investigate the possibility of reaction (iv), the C=C hydrogenation of CH_2=$CHCH_2CH_2OH$ was calculated by means of a concerted hydrogen transfer. Figure 10 shows that it is exergonic by 20.7 kcal/mol for **1** + CH_2=$CHCH_2CH_2OH$ → **14**, which is a thermodynamically feasible reaction. However, the total free energy barrier is 27.6 kcal/mol, which is only 0.5 kcal/mol lower than in reaction (i). According to the Eyring equation, the rate constant k_1 of reaction (iv) is 3.64×10^{-8} M^{-1} s^{-1} at room temperature. In experiments, it was found that $PhCOCH_3$ (1.5 mmol) with a $k_2 \approx 9.8 \times 10^{-3}$ M^{-1} s^{-1} needed ~20 h to finish the hydrogenation under reaction conditions of Knölker's catalyst **1** (30 μmol, 2.0 mol % catalyst), toluene (5 mL), and 3 atm H_2 at 25 °C. In comparison, reaction (iv) required a very long time (roughly estimated to be 5.0×10^6 h) to complete hydrogenation at a high temperature. This prediction shows that C=C is not able to be hydrogenated by Knölker's catalyst at room or low temperature, which is in good agreement with the experimental results of Casey and Guan.[24]

As stated previously, the high chemoselectivity of Knölker's iron catalyst for the hydrogenation of CH_2=$CHCH_2CHO$ can be attributed mainly to the large kinetic difference between the hydrogen transfer of the olefin and carbonyl. This is because two migrating hydrogen atoms of Knölker's catalyst exhibit strong polarization, where one is a proton and the other a hybrid ion. Thus, Knölker's iron catalyst prefers to catalyze the hydrogenation of polar substrates like ketones, aldehydes, and imines at low temperatures. For nonpolar substrates such as olefins and alkynes, it is necessary to increase the temperature to achieve catalytic hydrogenation. This feature of Knölker's catalyst can be effectively used to selectively catalyze the hydrogenation of many ketones, aldehydes, and imines with isolated C=C or C≡C groups.

CONCLUSIONS

The high chemoselectivity of Knölker's iron catalyst for the hydrogenation of CH_2=$CHCH_2CHO$ was studied in detail using DFT. Free energy profiles including solvation effects in toluene were calculated for all possible pathways. On the basis of our calculated results, the inner-sphere route involving the C=C bond binding to the iron is kinetically impossible for Knölker's iron-complex-catalyzed hydrogenation of olefins. By comparison, an outer-sphere pathway (no coordination) is the best kinetically available route. However, the hydrogenation of the C=C bond of 1-butenal has a high free energy barrier of 28.1 kcal/mol, which can be overcome only at very high temperature. Reactions (i) and (ii) cannot occur in the presence of Knölker's catalyst at room temperature, because the hydrogenation of the olefin is kinetically unfeasible. In this case, only reaction (iii) is kinetically available at room temperature due to a low free energy barrier of 14.0 kcal/mol. The high chemoselectivity of Knölker's iron catalyst can be mainly attributed to the different hydrogenation speeds of the C=C and C=O bonds. Thus, Knölker's catalyst can effectively and selectively catalyze the hydrogenation of polar groups in the substrate such as ketones, aldehydes, and imines, but not in nonpolar groups (like isolated C=C, cycloalkenyl, or C≡C groups).

COMPUTATIONAL DETAILS

Calculations for all geometries were carried out using the Gaussian 09 software package.[33] Optimizations were performed at the density functional theory (DFT) level by means of the hybrid B3LYP[34] functional and LACVP* basis set. The effective core potential LANL2DZ[35] along with its associated basis set was employed for Fe, and the main group elements (C, O, H, and Si) were calculated using the 6-31G* basis set. The structural parameters for Knölker's iron catalyst, 2,5-$(SiMe_3)_2$-3,4-$(CH_2)_4$(η^5-C_4COH)$Fe(CO)_2H$, **1**, used in all calculations were obtained based on its X-ray crystal structure.[25c]

All calculations were done without freezing any atom. Frequency calculations were performed for all stationary points at the same level to identify the minima (zero imaginary frequency) and transition states (TS, only one imaginary frequency) and to provide free energies at 298.15 K and 1 atm. Intrinsic reaction coordinate (IRC)[36] analysis was carried out to confirm that all stationary states were smoothly connected to each other. Solvent effects (in toluene) were included using the SMD model[37,38] with the M06 method (as implemented in Gaussian 09) by performing single-point calculations via the B3LYP-optimized geometries at the higher level of basis set, where the def2-TZVP[39] was employed for Fe and the 6-31++G** was used for main group elements. Zhao and Truhlar[40,41] reported that the M06 method has a high accuracy for the calculation of the thermochemistry and kinetics of transition metals and main-group elements.

A correction term of 1.8943 kcal/mol must be added to the G(sol) calculations to convert the gas-phase standard free energies at a standard state of 1 atm to the appropriate standard state for a solution of 1 mol/L.[42,43] Because the iron-catalyzed hydrogenation of ketones is a bimolecular reaction, the transition state can cause an entropy penalty in this step. So solvation free energies ΔG(sol) were used to evaluate the chemoselective capability of iron catalyst in this paper, in order to consider both entropic and solvent effects.

ASSOCIATED CONTENT

Supporting Information

Total electronic energies, thermal corrections to Gibbs free energies and Cartesian coordinates, and additional data. This material is available free of charge via the Internet at http://pubs.acs.org.

AUTHOR INFORMATION

Corresponding Authors

*E-mail: zhangmt@nankai.edu.cn.
*E-mail: sxmwch@sdu.edu.cn.

Notes

The authors declare no competing financial interest.

ACKNOWLEDGMENTS

We thank the National Natural Science Foundation of China (No. 21277082) for research funding.

REFERENCES

(1) Noyori, R. *Asymmetric catalysis in organic synthesis*; Wiley: New York, 1994.

(2) (a) Karvemu, R.; Prabhakaran, R.; Natarajan, K. *Coord. Chem. Rev.* **2005**, *249*, 911−918. (b) Gladiali, S.; Alberico, E. *Chem. Soc. Rev.* **2006**, *35*, 226−236.

(3) (a) Gomez, M.; Jansat, S.; Muller, G.; Aullon, G.; Maestro, M. A. *Eur. J. Inorg. Chem.* **2005**, *18*, 4341−4351. (b) Ito, M.; Hirakawa, M.; Murata, K.; Ikariya, T. *Organometallics* **2001**, *20*, 379−381.

(c) Abdur−Rashid, K.; Clapham, S. E.; Hadzovic, A.; Harvey, J. N.; Lough, A. J.; Morris, R. H. *J. Am. Chem. Soc.* **2002**, *124*, 15104−15118.
(4) (a) Wu, X.; Vinci, D.; Ikariya, T.; Xiao, J. *Chem. Commun.* **2005**, *35*, 4447−4449. (b) Clapham, S. E.; Morris, R. H. *Organometallics* **2005**, *24*, 479−481. (c) Martin, M.; Sola, E.; Tejero, S.; Andres, J. L.; Oro, L. A. *Chem.—Eur. J.* **2006**, *12*, 4043−4056. (d) Mao, J.; Baker, D. C. *Org. Lett.* **1999**, *1*, 841−843.
(5) Conley, B. L.; Pennington−Boggio, M. K.; Boz, E.; Williams, T. J. *Chem. Rev.* **2010**, *110*, 2294−2312.
(6) Fehring, V.; Selke, R. *Angew. Chem., Int. Ed.* **1998**, *37*, 1827−1830.
(7) Shvo, Y.; Czarkie, D.; Rahamim, Y.; Chodosh, D. F. *J. Am. Chem. Soc.* **1986**, *108*, 7400−7402.
(8) Shvo, Y.; Goldberg, I.; Czierkie, D.; Reshef, D.; Stein, Z. *Organometallics* **1997**, *16*, 133−138.
(9) Menashe, N.; Salant, E.; Shvo, Y. *J. Organomet. Chem.* **1996**, *514*, 97−102.
(10) Samec, J. S. M.; Bäckvall, J. E. *Chem.—Eur. J.* **2002**, *8*, 2955−2961.
(11) Csjernyk, G.; Éll, A. H.; Fadini, L.; Pugin, B.; Bäckvall, J. E. *J. Org. Chem.* **2002**, *67*, 1657−1662.
(12) (a) Samec, J. S. M.; Éll, A. H.; Bäckvall, J. E. *Chem.—Eur. J.* **2005**, *11*, 2327−2334. (b) Éll, A. H.; Samec, J. S. M.; Brasse, C.; Bäckvall, J. E. *Chem. Commun.* **2002**, *10*, 1144−1145.
(13) (a) Larsson, A. L. E.; Persson, B. A.; Pugin, B.; Bäckvall, J. E. *Angew. Chem., Int. Ed.* **1997**, *36*, 1211−1212. (b) Persson, B. A.; Larsson, A. L. E.; Ray, M. L.; Bäckvall, J. E. *J. Am. Chem. Soc.* **1999**, *121*, 1645−1650. (c) Paetzold, J.; Bäckvall, J. E. *J. Am. Chem. Soc.* **2005**, *127*, 17620−17621.
(14) Junge, K.; Schröder, K.; Beller, M. *Chem. Commun.* **2011**, *47*, 4849−4859.
(15) (a) Johnson, T. C.; Morris, D. J.; Wills, M. *Chem. Soc. Rev.* **2010**, *39*, 81−88. (b) Navarro, R. M.; Peña, M. A.; Fierro, J. L. G. *Chem. Rev.* **2007**, *107*, 3952−3991. (c) Turner, J. A. *Science* **2004**, *305*, 972−974.
(16) Bailly, B. A. F. L.; Thomas, S. P. *RSC Adv.* **2011**, *1*, 1435−1445.
(17) Goldschmidt, V. W. *Geochemistry*; Oxford Press: London, 1958; p 647.
(18) (a) Blaser, H. U.; Malan, C.; Pugin, B.; Spindler, F.; Steiner, H.; Studer, M. *Adv. Synth. Catal.* **2003**, *345*, 103−151. (b) Quintard, A.; Rodriguez, J. *Angew. Chem., Int. Ed.* **2014**, *53*, 4044−4055. (c) Li, Y.; Yu, S.; Wu, X.; Xiao, J.; Shen, W.; Dong, Z.; Gao, J. *J. Am. Chem. Soc.* **2014**, *136*, 4031−4039. (d) Quintard, A.; Constantieux, T.; Rodriguez, J. *Angew. Chem., Int. Ed.* **2013**, *52*, 12883−12887.
(19) Rylander, P. N. In *Hydrogenation Methods*; Academic Press: New York, 1990.
(20) (a) Bianchini, C.; Meli, A.; Peruzzini, M.; Vizza, F.; Zanobini, F.; Frediani, P. *Organometallics* **1989**, *8*, 2080−2082. (b) Bianchini, C.; Meli, A.; Peruzzini, M.; Frediani, P.; Bohanna, C.; Esteruelas, M. A.; Oro, L. A. *Organometallics* **1992**, *11*, 138−145.
(21) Bianchini, C.; Farnetti, E.; Graziani, M.; Peruzzini, M.; Polo, A. *Organometallics* **1993**, *12*, 3753−3761.
(22) Bohr, M. D.; Panda, A. G.; Jagtap, S. R.; Bhanage, B. M. *Catal. Lett.* **2008**, *124*, 157−164.
(23) Russell, S. K.; Darmon, J. M.; Lobkovsky, E.; Chirik, P. J. *Inorg. Chem.* **2010**, *49*, 2782−2792.
(24) Casey, C. P.; Guan, H. *J. Am. Chem. Soc.* **2007**, *129*, 5816−5817.
(25) (a) Knölker, H.-J.; Heber, J.; Mahler, C. H. *Synlett* **1992**, 1002−1004. (b) Knölker, H.-J.; Heber, J. *Synlett* **1993**, 924−926. (c) Knölker, H.-J.; Baum, E.; Goesmann, H.; Klauss, R. *Angew. Chem., Int. Ed.* **1999**, *38*, 2064−2066.
(26) Bart, S. C.; Lobkovsky, E.; Chirik, P. J. *J. Am. Chem. Soc.* **2004**, *126*, 13794−13807.
(27) Sylvester, K. T.; Chirik, P. J. *J. Am. Chem. Soc.* **2009**, *131*, 8772−8774.
(28) Zhang, H.; Chen, D.; Zhang, Y.; Zhang, G.; Liu, J. *Dalton Trans.* **2010**, *39*, 1972−1978.
(29) (a) Bart, S. C.; Hawrelak, E. J.; Schmisseur, A. K.; Lobkovsky, E.; Chirik, P. J. *Organometallics* **2004**, *23*, 237−246. (b) Bart, S. C.; Hawrelak, E. J.; Lobkovsky, E.; Chirik, P. J. *Organometallics* **2005**, *24*, 5518−5527. (c) Trovitch, R. J.; Lobkovsky, E.; Chirik, P. J. *Inorg. Chem.* **2006**, *45*, 7252−7260. (d) Bart, S. C.; Chlopek, K.; Bill, E.; Bouwkamp, M. W.; Lobkovsky, E.; Neese, F.; Wieghardt, K.; Chirik, P. J. *J. Am. Chem. Soc.* **2006**, *128*, 13901−13912. (e) Trovitch, R. J.; Lobkovsky, E.; Bill, E.; Chirik, P. J. *Organometallics* **2008**, *27*, 1470−1478.
(30) Lu, X.; Zhang, Y.; Yun, P.; Zhang, M.; Li, T. *Org. Biomol. Chem.* **2013**, *11*, 5264−5277.
(31) Chakraborty, S.; Dai, H. G.; Bhattacharya, P.; Fairweather, N. T.; Gibson, M. S.; Krause, J. A.; Guan, H. *J. Am. Chem. Soc.* **2014**, *136*, 7869−7872.
(32) (a) Lu, X.; Zhang, Y.; Turner, N.; Zhang, M.; Li, T. *Org. Biomol. Chem.* **2014**, *12*, 4361−4371. (b) Lu, X.; Zhang, Y.; Zhang, M.; Li, T. *J. Organomet. Chem.* **2014**, *749*, 69−74.
(33) Frisch, M. J., et al. Gaussian 09, Revision B.01; Gaussian, Inc.: Wallingford, CT, 2009.
(34) (a) Becke, A. D. *J. Chem. Phys.* **1993**, *98*, 5648−5652. (b) Lee, C.; Yang, W.; Parr, R. G. *Phys. Rev. B* **1988**, *37*, 785−789. (c) Stephens, P. J.; Devlin, F. J.; Chabalowski, C. F.; Frisch, M. J. *J. Phys. Chem.* **1994**, *98*, 11623−11627.
(35) (a) Hay, P. J.; Wadt, W. R. *J. Chem. Phys.* **1985**, *82*, 270−283. (b) Hay, P. J.; Wadt, W. R. *J. Chem. Phys.* **1985**, *82*, 299−310.
(36) (a) Fukui, K. *J. Phys. Chem.* **1970**, *74*, 4161−4163. (b) Fukui, K. *Acc. Chem. Res.* **1981**, *14*, 363−368.
(37) Marenich, A. V.; Cramer, C. J.; Truhlar, D. G. *J. Phys. Chem. B* **2009**, *113*, 4538−4543.
(38) Marenich, A. V.; Cramer, C. J.; Truhlar, D. G. *J. Phys. Chem. B* **2009**, *113*, 6378−6396.
(39) Xu, X.; Truhlar, D. G. *J. Chem. Theory Comput.* **2012**, *8*, 80−90.
(40) Zhao, Y.; Truhlar, D. G. *Acc. Chem. Res.* **2008**, *41*, 157−167.
(41) Zhao, Y.; Truhlar, D. G. *Theor. Chem. Acc.* **2008**, *120*, 215−241.
(42) Pratt, L. M.; Merry, S.; Nguyen, S. C.; Quan, P.; Thanh, B. T. *Tetrahedron* **2006**, *62*, 10821−10828.
(43) Pratt, L. M.; Truhlar, D. G.; Cramer, C. J.; Kass, S. R.; Thompson, J. D.; Xidos, J. D. *J. Org. Chem.* **2007**, *72*, 2962−2966.